Chinese Physics Letters

PAPER

Approach to Single-Mode Dominated Resonant Emission in GaN-Based Square Microdisks on Si*

CHIN. PHYS. LETT. Vol. 37, No. 5 (2020) 054204

Approach to Single-Mode Dominated Resonant Emission in GaN-Based Square Microdisks on Si *

Meng-Han Liu(刘梦涵)[1], Peng Chen(陈鹏)[1**], Zi-Li Xie(谢自力)[1], Xiang-Qian Xiu(修向前)[1], Dun-Jun Chen(陈敦军)[1], Bin Liu(刘斌)[1], Ping Han(韩平)[1], Yi Shi(施毅)[1], Rong Zhang(张荣)[1**], You-Dou Zheng(郑有炓)[1], Kai Cheng(程凯)[2], Li-Yang Zhang(张丽阳)[2]

[1] *Jiangsu Provincial Key Laboratory of Advanced Photonic and Electronic Materials and School of Electronic Science and Engineering, Nanjing University, Nanjing 210093*

[2] *Enkris Semiconductor Inc. NW-20, Nanopolis Suzhou, Suzhou 215123*

(Received 27 February 2020)

Square microdisks with round corners are fabricated using a standard GaN-based blue LED on Si substrates. Whispering gallery-like modes in the square microdisks are investigated by finite-difference time-domain simulation. The simulation results reveal that the round corners in square microdisks can substantially suppress the number of light propagation paths and further reduce the number of optical modes. A confocal micro-photoluminescence is performed to analyze the optical properties of the square microdisks at room temperature. The single-mode dominant resonant emission is obtained in the square microdisk with corner radius of 1.5 μm.

PACS: 42.55.Sa, 42.60.Da, 81.05.Ea DOI: 10.1088/0256-307X/37/5/054204

Optical microcavities, which confine light inside the gain material to enhance light-matter interactions, have attracted extensive attention in the past decades.[1−3] Generally speaking, the configurations of microcavities can be divided into Fabry–Pérot (F-P) microcavities,[4,5] distributed feedback (DFB) microcavities,[6,7] photonic crystal microcavities and whispering gallery mode (WGM) microcavities.[8−10] Among all these configurations, WGM microcavities, in which the photon localization is formed by the total internal reflection, can offer low threshold lasing by the virtue of high quality factor and small cavity volume.[11] Spatial and spectral controllable single-mode operation in the WGM microcavities is highly desirable in many applications, such as add-drop filter, chip-level integration and single-source optical communication.[12−14] In recent years, several effective mode control and selection strategies have been employed to obtain single-mode operation, such as parity-time (PT) symmetry breaking and coupled-asymmetric microcavity structure.[15,16] However, these methods of achieving single-mode operation put forward technological challenges because they make high demands on structural design and fabrication processes. In addition, most research on single-mode operation has been based on circular microcavities.[17,18] The circular microcavities have a large number of closely spaced WGMs, which makes them technical difficult in mode control and selection.

According to previous studies, the light propagation paths of the modes in square microcavities are confined along regular and isolated orbits, which is benefit for effective mode control and selection. More importantly, the free spectral range of the high Q modes in square microcavities is twice the one in the circular microcavities with similar sizes.[19,20] Thus, square microcavities are potential candidates for realizing single-mode operation. GaN and its group-Ⅲ nitrides are typical wide bandgap semiconductor materials. The interests on GaN-based microcavities lie in their irreplaceable and efficient blue-UV luminescence capability. Since the GaN-based circular microdisks on Si substrates were successfully fabricated by Choi *et al.*[10] in 2006, a large number of GaN-on-Si microdisks have emerged. The GaN-based microdisks on Si substrates can be potentially used to integrate with Si electronics, which promotes the development of optoelectronic integrated circuits. Although the GaN-on-Si circular microdisks have been widely studied, the single-mode resonant emission in GaN-on-Si square microdisks is far from being systematically studied.

In this Letter, we propose an approach to obtain single-mode dominated resonant emission in square microdisks. Finite-difference time-domain (FDTD) was introduced into the analysis of square microcavities to study electric field distributions of optical modes. Conventional top-down techniques

*Supported by the National Key R&D Program of China under Grant Nos. 2016YFB0400102 and 2016YFB0400602, the National Natural Science Foundation of China under Grant Nos. 61674076, 61422401, and 51461135002, the Collaborative Innovation Center of Solid State Lighting and Energy-saving Electronics, Open Fund of the State Key Laboratory on Integrated Optoelectronics under Grant No. IOSKL2017KF03, the Natural Science Foundation for Young Scientists of Jiangsu Province under Grant No. BK20160376, the Research Funds from NJU-Yangzhou Institute of Opto-electronics, and the Research and Development Funds from State Grid Shandong Electric Power Company and Electric Power Research Institute.

**Corresponding author. Email: pchen@nju.edu.cn; rzhang@nju.edu.cn

were adopted to fabricate the GaN-based square microdisks. Scanning electron microscopy (SEM) and confocal micro-photoluminescence (μ-PL) were employed to analyze the optical properties of all microdisks.

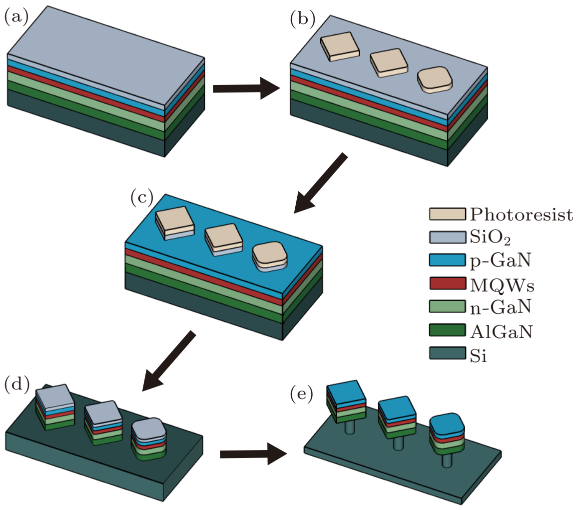

Fig. 1. Fabrication process of the square microdisk with different r. (a) SiO_2 deposition. (b) UV photolithography. (c) Reactive ion etching of SiO_2. (d) Inductively coupled plasma of GaN epitaxial layer. (e) Isotropic wet etchant of the Si substrate.

Square microdisks with undeformed corners are fabricated. Then, we fabricate square microdisks with round corners, the radii of round corners of the microdisks are $r = 0.75\,\mu m$ and $1.5\,\mu m$, respectively. The side length (L) of all fabricated square microdisks is $8.5\,\mu m$. The microdisks are made of a standard blue LED wafer grown on Si, which consists of $1.5\,\mu m$ AlGaN buffer layer, $1.5\,\mu m$ n-GaN layer, 6 pairs of InGaN/GaN MQWs and a 160-nm-thick p-GaN layer. The total thickness is $3.3\,\mu m$ approximately. The usage of the standard LED epitaxial wafer promotes the further development of electrically pumped lasing and commercial application. The square microdisks are fabricated by combining photolithography with the simple dry etching technique, and the undercut structure of the microdisks is formed by wet etching. The fabrication process is schematically depicted in Fig. 1. First, a SiO_2 mask layer is deposited on the surface of the p-GaN layer by plasma enhanced chemical vapor deposition (Fig. 1(a)). Then, a square microdisk with undeformed corners and two square microdisks with $r = 0.75\,\mu m$ and $1.5\,\mu m$ are patterned on the SiO_2 film using UV photolithography (Fig. 1(b)). Next, reactive ion etching is employed to etch the SiO_2 hard mask (Fig. 1(c)) and inductively coupled plasma dry etching is adopted to etch the GaN epitaxial layer (Fig. 1(d)). Finally, the sample is immersed in an HNO_3, HF and H_2O isotropic wet etchant to form the undercut structure (Fig. 1(e)).

The optical characteristics of the microdisks are measured by confocal micro-photoluminescence with the sample excited by a mode-locked Ti:sapphire pulsed laser ($\lambda_{pump} = 375\,nm$, pulse width 115 fs, repetition rate 76 MHz). The emission signal is detected by a Renishaw inVia Reflex micro-photoluminance spectroscopy system. All of the measurements are performed at room temperature.

Figure 2 shows the SEM images of the selected microdisk with different r. Limited by UV photolithography processes, the undeformed microdisk also shows small round corners. The r value of the small round corners is about $0.3\,\mu m$. Top-view images of the microdisks with different r are shown in Figs. 2(a)–2(c), revealing well-defined square boundaries with long flat sides and round corners. The side-view image of the microdisk with $r = 1.5\,\mu m$ is shown in Fig. 2(d). The side-view image reveals the presence of a square microdisk with a large air gap beneath the disk and a smooth outer surface. The large air gap ensures effective light confinement along the vertical direction. The smooth outer surface, especially the smooth sidewall, is crucial to achieving the excellent performance of microdisks because any roughness may cause a scattering of light and a leakage of optical modes. It can be seen that the sidewall of the microdisk is slightly tilted. The thickness of the disk region is $3.3\,\mu m$, approximately.

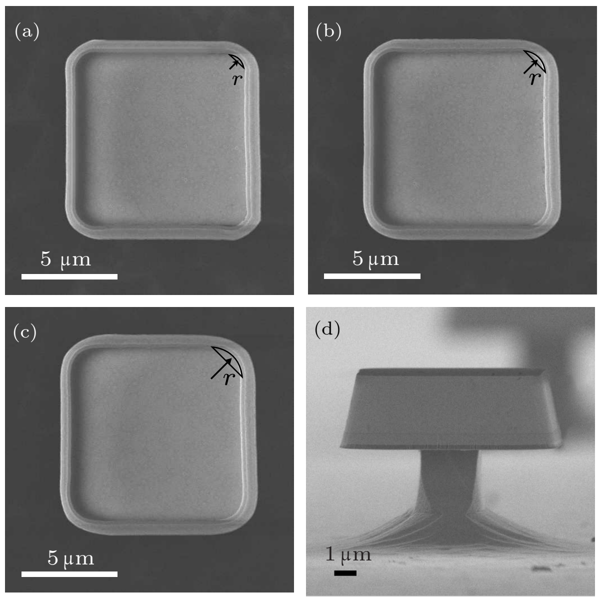

Fig. 2. Top-view of microdisks with $r = 0.3\,\mu m$ (a), $0.75\,\mu m$ (b) and $1.5\,\mu m$ (c). Side-view SEM images of the square microdisk with $r = 1.5\,\mu m$ (d).

To investigate the influence of round corners on mode characteristics, 2D-FDTD analysis is proposed to simulate the spectral intensity and radial electric field distributions of square microcavities with different r. According to the material properties, the TM polarized emission is much weaker than TE polarized emission in GaN material systems, so only the characteristics of TE modes are investigated. The spectral intensity obtained by simulation in the square microcavities with different r is plotted in Fig. 3. The number of emission peaks decreases as r increases. Single-mode emission is achieved in the square microcavity with $r = 1.5\,\mu\text{m}$.

The radial electric field distributions $|E|$ of optical modes with the highest Q factor in the square microcavities are shown in Fig. 4. The tilted sidewall of microdisk shown in Fig. 2(d) has significant influences on the axial electric field distributions rather than the radial electric field distributions. The mode is confined in the square microcavity by total internal reflection, which is known as whispering-gallery-like mode.[21] In contrast from WGMs trapped along the periphery of a circular microcavity, the whispering-gallery-like modes in the square microcavity spread through the whole cavity. Thus, the surface defects caused by dry etching have less influence on the square microdisks than on the circular microdisks. In addition, the light propagation paths of the optical modes in the square microcavities are confined along isolated rectangular orbits.

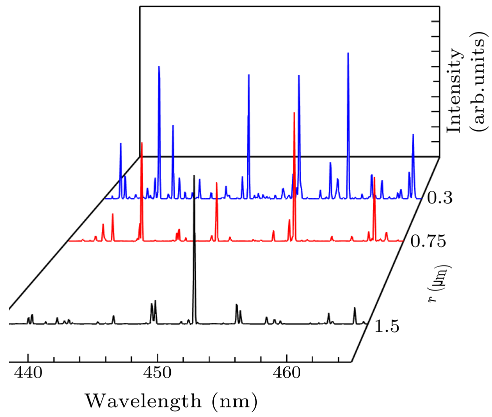

Fig. 3. Intensity spectra obtained by the FDTD simulation in square microdisks with different r.

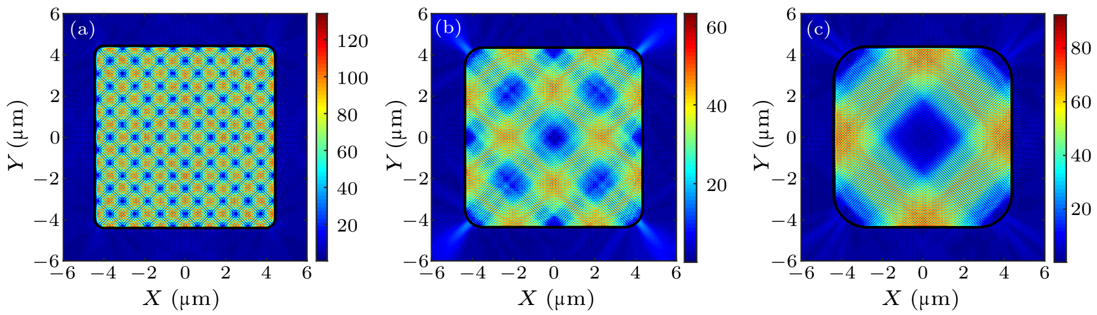

Fig. 4. Electric field distributions $|E|$ of optical modes with the highest Q factor in the square microcavities with (a) $r = 0.3\,\mu\text{m}$, (b) $r = 0.75\,\mu\text{m}$, and (c) $r = 1.5\,\mu\text{m}$.

The electric field profile of square microcavity with $r = 0.3\,\mu\text{m}$ is shown in Fig. 4(a), which reveals that there are a lot of light paths propagating over the whole cavity region. The electric field profile of microcavity with $r = 0.75\,\mu\text{m}$ is shown in Fig. 4(b). Compared with the microcavity with $r = 0.3\,\mu\text{m}$, light propagation paths trapped along rectangular orbits in this microcavity are obviously reduced. As r increases to $1.5\,\mu\text{m}$, the number of light propagation paths is further reduced and the fundamental TE mode is shown in Fig. 4(c). Although the electric field distributions are typically weak at the corners, light scattering from the round corners can be clearly observed. According to the simulation results of FDTD, the number of light propagation paths confined in the deformed microcavities is substantially reduced as the increase of r.

To obtain a single mode resonant emission, we fabricate the square microdisks with $r = 0.3\,\mu\text{m}$, $0.75\,\mu\text{m}$ and $1.5\,\mu\text{m}$, respectively. Figure 5 shows the PL spectral evolution of the resonant emission from the selected microdisks. A broad spontaneous emission spectrum centered at 451 nm is observed at low pump power. When the threshold is exceeded, a series of sharp peaks appear and are superimposed on the spontaneous emission envelop. As pump power further increases, these sharp peaks become stable. This is typical behavior of resonant emission. The plots of integrated PL spectra intensity with pump power are shown in Figs. 5(d)–5(f). This nonlinear increase of the spectra intensity further indicates the resonant emission in the square microdisks. The threshold is identified as the kink of the curve. The thresholds of the three microdisks with $r = 0.3\,\mu\text{m}$, $0.75\,\mu\text{m}$ and $1.5\,\mu\text{m}$ are 5.897 mW, 5.401 mW, and 5.931 mW, respectively, which indicates that the deformed corners have little effect on the threshold. The threshold of microdisks is closely related to the area of the disk.[22] Since these square microdisks with different r have similar areas, they have similar thresholds. The Q factor can be calculated from the relation $Q = \lambda/\delta\lambda$, where λ and $\delta\lambda$ are the central wavelength and the full width at half maximum (FWHM) of the resonant peak, respectively. The Q factors for the three microdisks with $r = 0.3\,\mu\text{m}$, $0.75\,\mu\text{m}$ and $1.5\,\mu\text{m}$ are estimated to be about 320 ($\lambda = 451.65\,\text{nm}$), 390

(λ = 452.39 nm) and 520 (λ = 452.12 nm), respectively. Due to the absence of lasing, the Q factors are relatively low.

From the PL spectra of square microdisk with $r = 0.3\,\mu$m (Fig. 5(a)), there are two dominant resonant peaks at 449.25 nm and 451.65 nm, as well as a few secondary peaks at 444.14 nm and 446.27 nm. Once r increases to 0.75 µm (Fig. 5(b)), the PL spectra show a dominant resonant peak at 452.39 nm and a few secondary resonant peaks at 445.12 nm, 448.84 nm and 454.955 nm. When r increases to 1.5 µm (Fig. 5(c)), there is only one dominant resonant peak located at 452.12 nm and the secondary peaks are suppressed. The number of dominant resonant peaks decreases with the increase of r and the single-mode dominant resonant emission is obtained in the microdisk with $r = 1.5\,\mu$m, which is consistent with the calculation results.

For the square microcavity with round corners, the incident light at the curved corner is multiply reflected at the curved boundary and experiences severe scattering loss.[23] The scattered light cannot close upon themselves after several total internal reflections. Thus, the number of light propagation paths confined in the microcavities with round corners is substantially reduced. The decrease of light propagation paths further reduces the optical modes. The number of light propagation paths in square microcavity with $r = 0.75\,\mu$m is less than that in square microcavity with $r = 0.3\,\mu$m. Thus, the number of dominant resonant peak in square microdisk with $r = 0.75\,\mu$m is reduced. As r increase to 1.5 µm, only the light hitting at the middle parts of the sides can close upon themselves after several total internal reflections. The fundamental TE mode is achieved in the square microdisk with $r = 1.5\,\mu$m, as shown in Fig. 4(c). Thus, the single-mode dominated resonant emission has been obtained in the square microdisks with $r = 1.5\,\mu$m.

According to the PL spectra shown in Fig. 5, the microdisks are not driven hard enough to display clear laser action. The square microdisks made using a standard LED wafer are much thicker than those GaN-based microdisks that display lasing action.[24,25] More important, the LED wafer has a 160 nm p-GaN layer with a Mg doping concentration of $10^{20}\,\mathrm{cm}^{-3}$, which causes intensive impurity absorption. The extremely thick disk region and heavily doped top layer lead to the high optical loss, which is the main reason for the absence of lasing in square microdisks.

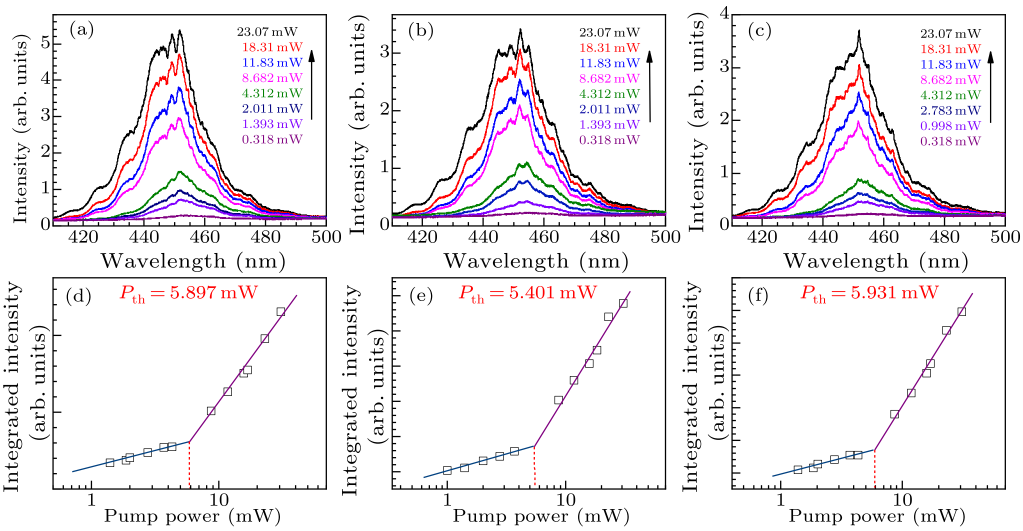

Fig. 5. Photoluminescence spectra from microdisks with $L = 8.5\,\mu$m for (a) $r = 0.3\,\mu$m, (b) $r = 0.75\,\mu$m, and (c) $r = 1.5\,\mu$m. The integrated PL spectra intensity versus pump optical power for microdisks with (d) $r = 0.3\,\mu$m, (e) $r = 0.75\,\mu$m, and (f) $r = 1.5\,\mu$m.

In conclusion, we propose an approach to obtain single-mode dominated resonant operation in the GaN-based square microdisks. According to FDTD simulation, the scattering loss from the round corners reduces the number of light propagation paths, as well as the optical modes. The single-mode dominated resonant emission has been obtained in the square microdisk with round corners radius of $r = 1.5\,\mu$m. From the numerical and experimental results, we can draw the conclusion that rounding the corners of a GaN-based square microdisk is an effective way to achieve single-mode operation. With the simple fabrication process and resonator structure, the single-mode resonant characteristics in the square microdisks hold great promise for applications in quantum sciences and integrated photonic technologies.

References

[1] Jiang X F, Zou C L, Wang L, Gong Q H and Xiao Y F 2016

Laser & Photon. Rev. **10** 40
[2] He L N, Özdemir Ş K and Yang L 2013 *Laser & Photon. Rev.* **7** 60
[3] Min B, Ostby E, Sorger V, Ulin-Avila E, Yang L, Zhang X and Vahala K 2009 *Nature* **457** 455-U3
[4] Muller A, Flagg E B, Lawall J R and Solomon G S 2010 *Opt. Lett.* **35** 2293
[5] Dobrovolsky A, Stehr J E, Sukrittanon S, Kuang Y J, Tu C W, Chen W M M and Buyanova I A 2015 *Small* **11** 6331
[6] Wang M and Zhang X P 2017 *Nanoscale* **9** 2689
[7] Takeuchi H, Natsume K, Suzuki S and Sakata H 2007 *Electron. Lett.* **43** 30
[8] Nozaki K and Baba T 2004 *Appl. Phys. Lett.* **84** 4875
[9] Selles J, Crepel V, Roland I, El Kurdi M, Checoury X, Boucaud P, Mexis M, Leroux M, Damilano B, Rennesson S, Semond F, Gayral B, Brimont C and Guillet T 2016 *Appl. Phys. Lett.* **109** 231101
[10] Choi H W, Hui K N, Lai P T, Chen P, Zhang X H, Tripathy S, Teng J H and Chua S J 2006 *Appl. Phys. Lett.* **89** 211101
[11] Yang S C, Wang Y and Sun H D 2015 *Adv. Opt. Mater.* **3** 1136
[12] Qiang Z X, Zhou W D and Soref R A 2007 *Opt. Express* **15** 1823
[13] Xie W Q, Stöferle T, Rainò G, Aubert T, Bisschop S, Zhu Y P, Mahrt R F, Geiregat P, Brainis E, Hens Z and Van Thourhout D 2017 *Adv. Mater.* **29** 1604866
[14] Qualtieri A, Morello G, Spinicelli P, Todaro M T, Stomeo T, Martiradonna L, De Giorgi M, Quelin X, Buil S, Bramati A, Hermier J P, Cingolani R and De Vittorio M 2009 *New J. Phys.* **11** 033025
[15] Feng L, Wong Z J, Ma R M, Wang Y and Zhang X 2014 *Science* **346** 972
[16] Wu X, Li H, Liu L Y and Xu L 2008 *Appl. Phys. Lett.* **93** 081105
[17] Tang B, Sun L X, Zheng W H, Dong H X, Zhao B B, Si Q Q, Wang X X, Jiang X W, Pan A L and Zhang L 2018 *Adv. Opt. Mater.* **6** 1800391
[18] Zhu G Y, Li J P, Li J T, Guo J Y, Dai J, Xu C X and Wang Y J 2018 *Opt. Lett.* **43** 647
[19] Yang Y D and Huang Y Z 2016 *J. Phys. D* **49** 253001
[20] Guo W H, Huang Y Z, Lu Q Y and Yu L J 2004 *Chin. Phys. Lett.* **21** 79
[21] Yang Y D, Weng H Z, Hao Y Z, Xiao J L and Huang Y Z 2018 *Chin. Phys. B* **27** 114212
[22] Sellés J, Brimont C, Cassabois G, Valvin P, Guillet T, Roland I, Zeng Y, Checoury X, Boucaud P, Mexis M, Semond F and Gayral B 2016 *Sci. Rep.* **6** 21650
[23] Moon H J, Sun S P, Park G W, Lee J H and A N K 2003 *Jpn. J. Appl. Phys. Part 2 Lett.* **42** L652
[24] Tamboli A C, Haberer E D, Sharma R, Lee K H, Nakamura S and Hu E L 2007 *Nat. Photon.* **1** 61
[25] Athanasiou M, Smith R, Liu B and Wang T 2015 *Sci. Rep.* **4** 7250